Journal of Applied Polymer Science

Highly Scalable Nanoparticle–Polymer Composite Fiber via Wet Spinning

Roland Stone, Stephen Hipp, Joel Barden, Phillip J. Brown, O. Thompson Mefford
Department of Materials Science and Engineering, 161 Sirrine Hall, Clemson, South Carolina, 29634
Correspondence to: O. T. Mefford (E-mail: mefford@clemson.edu)

ABSTRACT: Magnetic nanoparticles have continued to gather the interest of researchers due to the unique physical properties of materials found at this size scale. Herein, the production of composite magnetic fibers composed of iron oxide nanoparticles suspended in alginate is described. These materials were produced via wet spinning of a sodium alginate solution into a bath of an aqueous solution of calcium chloride. The magnetic fibers were found to have similar mechanical properties to normal alginate fibers, and exhibited superparamagnetic behavior when subjected to an external DC magnetic field. In addition, the particle loaded fibers demonstrated the potential to produce significant amounts of heat when exposed to an AC magnetic field, suggesting these new materials could be applicable to a variety of applications including magnetic hyperthermia. © 2013 Wiley Periodicals, Inc. J. Appl. Polym. Sci. 130: 1975–1980, 2013

KEYWORDS: composites; colloids; fibers; magnetism and magnetic properties; nanoparticles; nanowires; nanocrystals

Received 18 December 2012; accepted 11 April 2013; Published online 10 May 2013
DOI: 10.1002/app.39408

INTRODUCTION

Magnetic nanoparticles have become an interdisciplinary tool that has found use in data storage,[1] biomedical imaging and treatment,[2] and catalysis.[3] Their size and surface chemistry allows for incorporation into composites to add a magnetic component that can be manipulated by an external magnetic field. One class of material that magnetic nanoparticles have found purpose in are polymeric fibers. These magnetic composite fibers can be involved in a variety of applications including biomedicine[4,5] and multiferroics.[5] The inclusion of magnetic nanoparticles in the fabrication of fibrous composites enables alignment of the fibers while spinning[6] or the potential of creating self-assembled magnetic nanoparticles structures.[7] Producing a polymer–particle composite by including the particles in the formation of the fiber allows for the addition of magnetic properties into a unique physical geometry, thus creating new opportunities for the application of these field responsive materials.

Several authors have produced polymer-magnetic particle fibers through a variety of techniques. For example, Turek et al.[8] were able to create a magnetic composite fiber from a polymer ferrofluid by stretching the viscous polymer solution in a magnetic field. This idea has advanced into the incorporation of magnetic nanoparticles (MNPs) into polymeric fibers via electrospinning. Two additional approaches for creating magnetic composite fibers include creating ferrofluid spinning solutions,[7] and coating the electrospun fiber surface with magnetic nanoparticles.[9] There has been little work done on incorporating magnetic nanoparticles into alginate or incorporating them into wet spinning processes. Wet spinning is a method that can be scaled easily and is commonly utilized in the high performance fiber industries for creating such materials as Twaron and Kevlar.[10] This method allows for the incorporation of unique filler materials into fibers of a variety of diameters and particle loading levels. This method can also utilize materials that cannot be processed using other spinning techniques. For example, melt-spinning of a polymer doped with MNPs will cause the particles to oxidize, thus reducing the magnetic response. Wet spinning magnetic nanoparticles into alginate is a more viable, higher throughput, and cost effective method over electrospinning or similar methods.

Sodium alginate is a polysaccharide composed of α-L-guluronic acid and β-D-mannuronic acid that is extracted from seaweed and is thus a renewable resource. This polysaccharide has been used for many years in the food, paper, and pharmaceutical industries.[11] Alginate fibers are generally produced via wet spinning sodium alginate in an aqueous solution into a calcium chloride bath where it then forms a gelatinous structure that can be drawn into a fiber. These fibers have found use in wound dressings because of its ability to accelerate healing by high absorption of fluid from the contusion.[12]

MNPs can be synthesized in many different ways, two methods most commonly used are thermal decomposition of metallic precursors in high boiling solvents[13] and the co-precipitation of metallic salts in high pH, aqueous solutions.[14] The preparation of MNPs by thermal decomposition allows for size control and a narrow range in sizes, unfortunately this method is conducted at high temperatures and can be challenging to scale up. This is untrue for synthesizing MNPs using co-precipitation of metallic salts. They can be synthesized in very large batches at room temperature, but control of size and polydispersity is limited. For some applications the scaling and cost of co-precipitation is very attractive for the creation of MNPs.

The objective of this study was to demonstrate that iron oxide magnetic nanoparticles (IONPs) could be incorporated into fibers using highly scalable methods of synthesizing particles and spinning fibers. This was successfully executed by scaling up a common procedure of precipitation of iron salts to create a suspension of water dispersed magnetic nanoparticles. This ferrofluid was then used to dissolve sodium alginate resulting in a spinning solution that was wet-spun into a calcium chloride bath.

EXPERIMENTAL

Characterization

TGA. Thermogravimetric analysis (TGA) was accomplished using a Hi-Res TGA 2950 thermogravimetric analyzer from TA Instruments. Experiments were controlled via Thermal Advantage Instrument Control Software (v 1.3.0.205) and thermogram was analyzed using TA Universal Analysis 2000 (v 3.9A, build 3.9.0.9). All samples where run with TA Instruments' platinum sample pans, 100 μL. The fiber samples were exposed to nitrogen for 20 min, followed by a ramp to 100°C at a rate of 20°C min^{-1}, held isothermally for 10 min, and then ramped to 700°C at a rate of 20°C min^{-1}.

Modulated DSC. Modulated differential scanning calorimetry (DSC) was used to determine the heat capacity of the alginate fibers doped with MNPs. Experiments were completed using a DSC Q1000 V9.9 Build 303 from TA Instruments. Samples were prepared by cutting the doped alginate fibers into small pieces and putting them into three DSC aluminum sample pans, each mass was less than 5 mg. A sapphire standard was first run from 0°C to 50°C to and the heat capacity found was compared to literature values. The three doped alginate fibers samples were run at the same temperature regime. All measurements were done under a helium purge, the temperature was brought to 0°C and then ramped to 50°C at a rate of 4°C min^{-1}, modulated ± 0.42°C min^{-1} every 40 s with an isothermal for 5 min at 50°C. The heat capacity was measured from 5 to 50°C and was found to have a mean value of 1.01 J g^{-1} K^{-1} with a standard deviation of 0.03 J g^{-1} K^{-1}.

TEM. Samples for transmission electron microscopy (TEM) were obtained by dropping diluted water solution onto a copper grid with carbon film. High-resolution TEM images were acquired at an accelerating voltage of 300 kV on a Hitachi H-9500.

DLS. Dynamic Light Scattering (DLS) was used to measure hydrodynamic radius using a Malvern Zetasizer Nano ZS (Model: ZEN3600). Measurements were controlled and analyzed with Dispersion Technology Software (DTS; v. 5.10). Size measurements for water dispersed particles were performed in Plastibrand® disposable cuvettes (Cat. No. 759070D).

Tensile Testing. Tensile testing was conducted using an Instron Model 5500R1125. Instron Bluehill (v 2.04) was used to collect data. Both fibers with and without nanoparticles were prepared by cutting five samples each, 10 cm in length.

VSM. Vibrating sample magnetometry (VSM) was accomplished with a VSM from Quantum Designs, on the physical property measurement system (PPMS) by wrapping 0.6 mg of fiber in Kapton tape and loading it onto the holder and putting it under vacuum (~10 Torr). The fiber was measured at 300 K over a field of ±3 T (±2387 kA m^{-1}) at a rate of 100 Oe s^{-1}. The background was obtained by submitting just the Kapton tape to the same procedure. The data presented in Figure 3 has the background subtracted from it.

AC Susceptibility. The real and imaginary susceptibility was measured using an IMEGO DynoMag system (hardware v. B, software v.B1g).The fiber sample, 0.5 g in 0.5 mL of water, was scanned over the a frequency range from 1 to 2,50,000 Hz and the volume susceptibility was collected versus frequency.

AC Magnetic Hyperthermia. Alternating current (AC) magnetic hyperthermia measurements were performed using an Ambrell Easy Heat from Ameritherm. A 5 mg sample of the fiber was placed in 0.5 mL of water in a sample chamber that was surrounded by a water jacket, kept at ~25°C via recirculating water bath, inside a five turn, 1/4″ I.D. copper coil. Temperature of the sample and the water jacket were monitored with an infrared thermocouple. Each sample was equilibrated in water jacket for 30 s before the AC field (41 kA m^{-1}, 150 kHz) was applied for 300 s. Time and temperature were recorded using a program created in National Instruments LabVIEW (v8.5.1). Each sample was analyzed in triplicate and an average heating rate was found. The initial heating rate was determined by applying a linear fit to the change in temperature over the first 30 s. Specific absorption rate (SAR), *eq.* (1), was calculated using a weighted average specific heat capacity of the doped alginate fiber (1.01 J g^{-1} K^{-1}) and water of 4.15 J g^{-1} K^{-1}. The SAR value is commonly used to describe the heating efficiency of composites used for magnetic hyperthermia. It describes the "power of heating of a magnetic material per gram," where C_v is the heat capacity of both the system, ΔT is the change in temperature, Δt is the change in time, and m_{iron} is the mass of iron in the sample.[15]

$$\mathrm{SAR} = C_v \left(\frac{\Delta T}{\Delta t} \right) m_{\mathrm{Iron}} \quad (1)$$

Incorporation of Magnetic Nanoparticles into Wet Spinning Materials. Ferric chloride, calcium chloride (Spectrum), ferrous chloride tetrahydrate (EMD), sodium hydroxide (50% w/w, VWR), sodium alginate (medium viscosity, Sigma Aldrich) were used as received.

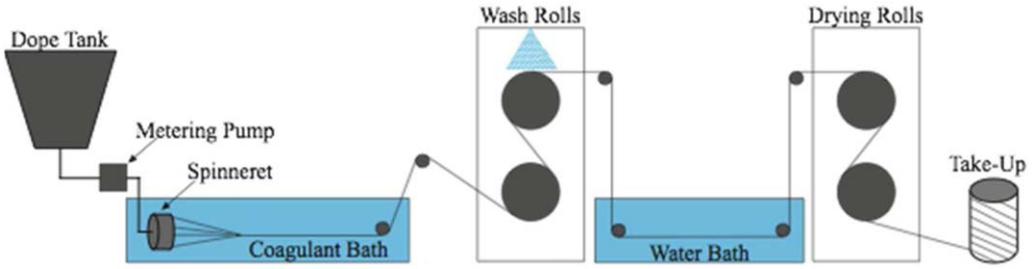

Figure 1. Schematic of wet spinning line used in production of magnetic fibers. [Color figure can be viewed in the online issue, which is available at wileyonlinelibrary.com.]

Particle Synthesis. Ferric chloride (114.193 g, 0.70 mol) and ferrous chloride (69.98 g, 0.35 mol) were dissolved in 530 mL of DI water and bubble with nitrogen for 45 min to deoxygenate the solutions. In a separate 12 L round bottom flask, 5.5 L of a 1.5*M* sodium hydroxide solution was bubbled with nitrogen for 45 min. Under a nitrogen purge, the solution of iron salts was slowly cannulated into sodium hydroxide solution while stirring under nitrogen purge. After stirring for 30 min, the final black solution was washed with DI water until a pH of 7.

Fiber Formation. The spinning solution was prepared by slowly adding sodium alginate (4% w/w) to nanoparticle solution in water (5% w/w) while stirring. Prior to spinning, the doped alginate solution was degassed for several hours under hard vacuum. Fiber samples were spun at a volumetric flow rate of 4 mL min^{-1} using an 80 hole, 150 μm spinneret into a coagulation bath consisting of a 15% (by weight) solution of calcium chloride in water. The fiber was taken up by the wash rolls at 5.5 m min^{-1}. The sample was then drawn at a 1.10 draw ratio through a hot water bath (∼70°C) before being collected on a package using a constant speed winder. Wet spinning schematic is displayed in Figure 1.

RESULTS AND DISCUSSION

The purpose of this project was to demonstrate that magnetically responsive fibers can be created via large scale production techniques. The particles synthesized, using the common methodology of the coprecipitation of iron salts, were analyzed with TEM and DLS. TEM [Figure 2(a)] shows the clustering and polydisperse nature that the coprecipitation method can produce and DLS [Figure 2(b)] showed that the particles have a hydrodynamic diameter of 196 nm by intensity suggesting that the particles formed are largely agglomerated, which is common for particle synthesis of this nature. The fibers spun (Figure 3) are a deep black in color, indicating that the coprecipitation nanoparticles were dispersed throughout the fiber. It was also observed that over time there was no visual oxidation of the nanoparticles once they were imbedded into the fiber.

To observe how the particles were dispersed in the fiber, TEM micrographs were taken of a longitudinal slice of the magnetic fiber, shown in Figure 4. The particles were successfully encapsulated into the fiber with none visibly on the surface [Figure 4 (a)]. Linear aggregates of the particles were formed in a variety shapes and sizes along direction of formation. The agglomerates were much larger than those observed in the TEM of the coprecipitation nanoparticles before they were added to alginate [Figure 2(a)]. These agglomerations have potential to affect mechanical and magnetic properties of the fibers that are discussed further in this section.

Tensile testing was conducted on the alginate fiber with and without MNPs using an Instron to measure the elongation,

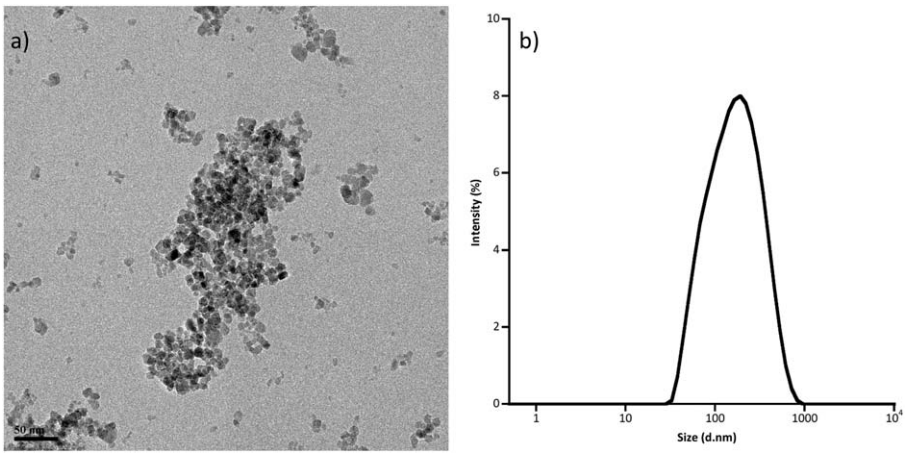

Figure 2. (a)TEM and (b)DLS of IONP synthesized by coprecipitation. Scale bar has a width of 50 nm.

Applied Polymer SCIENCE

Figure 3. Bobbin of spun alginate doped with IONP. [Color figure can be viewed in the online issue, which is available at wileyonlinelibrary.com.]

tenacity, and modulus, as shown in Table I. This method was used to observe any changes in the physical properties that may manifest from MNP doping. Although the values are low, there was no significant difference observed in elongation, tenacity, and modulus that would be inherited when creating composites. Statistical analysis was done to confirm that there was no significant difference between the two fibers. The probability was calculated using a *t*-test to compare the two data sets. The values found for elongation ($t = 1.51$, $p = 0.21$), tenacity ($t = -1.37$, $p = 0.24$), and modulus ($t = -0.81$, $p = 0.46$) all with four degrees of freedom. With reasonable confidence there is no significant difference between the mechanical properties of the alginate fiber and the doped alginate fiber.

TGA was used to measure the mass fraction loading of particles within the fiber by comparing the difference between the char yields of the alginate fiber and a doped alginate fiber (Figure 5). By accounting for the char yield of the doped alginate (42.5 %), char yield of magnetite (94.0%), and char yield of alginate fiber (52.6%), the mass fraction of iron oxide in the fiber was calculated to be 19.6% and the volume fraction to be 7%, using the density for alginate of 1.6 g mL^{-1} and density for bulk magnetite of 5.18 g mL^{-1}. In Figure 4, there is no more weight loss observed for the coprecipitation MNPs after 285°C, so any weight in this region is due to the degradation of alginate. The difference in the weight loss profiles between alginate fiber with MNPs and without is likely due to the interactions and difference in density between the alginate and IONPs. In the initial step that begins at about 220°C, the alginate fiber with MNPs starts to lose weight at a higher temperature compared to the alginate in the fiber. This is due to the high density of the particles embedded in the alginate and possible interactions between the free alcohols of the alginate, delaying the decomposition temperature of the alginate in the fiber. Although the initial degradation of alginate with MNPs is delayed compared to the non-doped alginate fiber, each step preceding is shifted to a lower temperature. There is less alginate per filament in the alginate fiber with MNPs, about 19.6% by mass, so degradation will occur at a lower temperature.

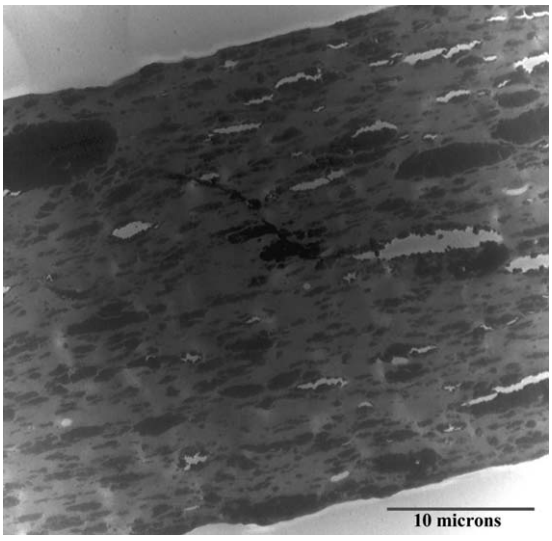

Figure 4. TEM micrograph of a slice along the length of the fiber.

Table I. Tensile Testing of Alginate Fibers and Doped Alginate Fibers

	Alginate fiber	Doped alginate
Denier	529	508
Elongation (%)	4.22 ± 1.18	5.33 ± 1.10
Tenacity (g den^{-1})	0.68 ± 0.07	0.63 ± 0.03
Modulus (g den^{-1})	19.02 ± 3.04	17.73 ± 0.63

The magnetic behavior of the doped fiber was measured at room temperature with a VSM. The magnetization curve [Figure 6(b)] illustrates that the fiber does display superparamagnetic behavior at room temperature as there is no significant remanent magnetism or coercivity observed.[16] Susceptibility was measured using AC susceptometry [Figure 6(a)]; the results confirm that there is a magnetic response in an AC magnetic field, as seen with materials that display superparamagnetic properties. Unfortunately, high enough frequencies could not be

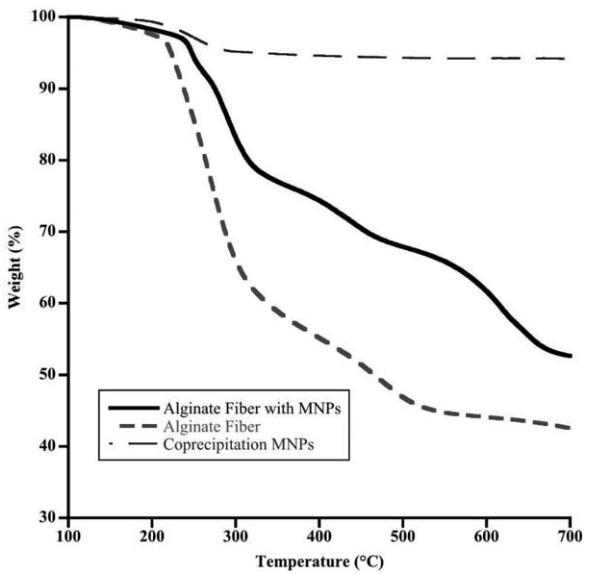

Figure 5. TGA of alginate fiber, doped alginate fiber, and coprecipitation MNPs.

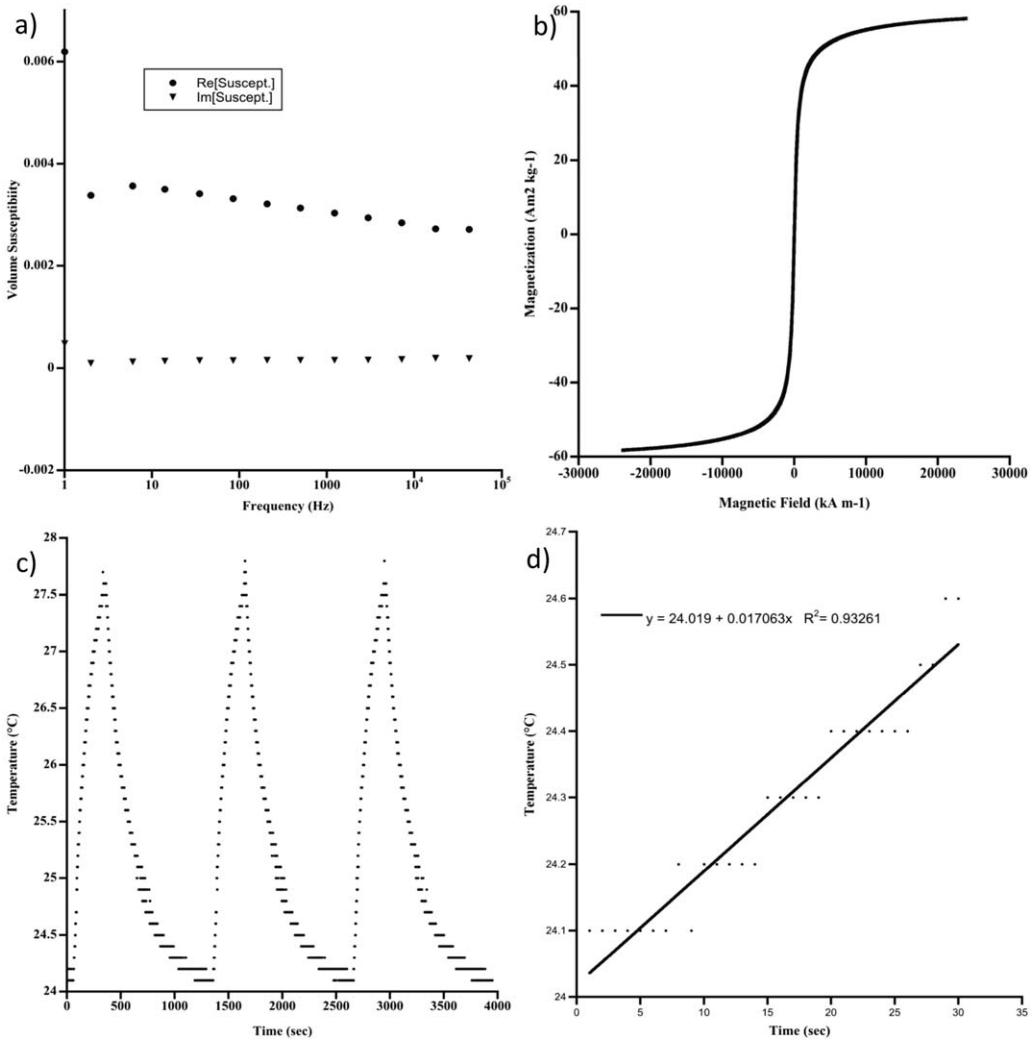

Figure 6. (a) Real and imaginary susceptibility of alginate doped with IONPs. (b) VSM of alginate doped with iron oxide nanoparticles at 300 K. (c) Temperature profile of magnetic fiber from repeated heating. (d) Initial heating rate of alginate doped with IONPs using AC field.

reached with the instrument to extrapolate how these particles are colloidally arranged within the fiber.

Since the fibers produced were shown to exhibit magnetic properties with VSM and AC susceptometry, they were placed in an AC magnetic field to see if heating would be possible via methods employed for magnetic hyperthermia of ferrofluids. Magnetic hyperthermia is an experimental technique for the treatment of cancer in which AC magnetic fields are used to induce the heating of magnetic nanoparticles yielding a localized fever to promote death of tumor cells. The fibers were subjected to the same field and frequency three consecutive times, shown in Figure 6(c). There was no observed difference in maximum temperature reached between experiments, demonstrating that the fiber can consistently heat the surrounding water at the same rate and there are no changes in the magnetic response following the cycles. The water surrounding the magnetic fibers rose from 24°C to almost 28°C after 300 s, with the initial heating rate [Figure 6(d)] to be almost 0.02°C s^{-1}. The heat capacity of the magnetic fiber was measured over a range of 5 to 50°C and was found to be 1.01 J g^{-1} K^{-1} with a standard deviation of 0.03 J g^{-1} K^{-1}. The heat capacity of the magnetic fiber in water was calculated using a weighted average heat capacity. Although only 0.01% by weight of the sample was the magnetic fiber, the weighted average heat capacity (C_p) does decrease the heat capacity of water (4.18 J g^{-1} K^{-1}) to 4.15 J g^{-1} K^{-1}. Using the aforementioned calculated heat capacity of the sample, a temperature change of 0.6°C over the first 30 s, and 0.71 mg of iron in the fiber found from TGA, the specific absorption rate (SAR) was calculated to be 116.9 W g^{-1}. Unfortunately, it is difficult to compare this value to other ferrofluids used for magnetic hyperthermia because of the variability of field, frequency, and intrinsic properties that differ between samples. For example, SAR was measured on iron nanoparticles in a gel suspension and found to be 25 W g^{-1} at a similar field and frequency, but had a much higher concentration of iron, 7.24 mg.[17]

CONCLUSIONS

Magnetic nanoparticle synthesis is easily scalable when using the coprecipitation of iron salts. Because these particles were already

dispersed in an aqueous solution, adding sodium alginate to create a spinning solution was easily accomplished. The fiber was wet spun, similarly to that done in industry, without modifying the traditional wet spinning line. When studying the magnetic properties of these fibers, there was evidence of superparamagnetic behavior at room temperature. This behavior allows for magnetic manipulation of the material in a magnetic field, but when removed, the material exhibits very little remanence.

These fibers were subjected to an AC magnetic field and observed a change in temperature over time. Measuring the change in temperature in a ferrofluid is a common characterization technique for systems used in magnetic hyperthermia. The fibers did exhibit heating when exposed to an AC field, with a rate of 0.02°C s^{-1} and a SAR of 116.9 W g^{-1}. The heat capacity used in calculating the SAR was a weighted average of the fiber and water. The heat capacity of the fiber was found to be 1.01 J g^{-1} K^{-1} from 5 to 50°C using modulated DSC. The SAR found in our system is difficult to accurately compare to literature because of the variability between AC calorimeter instruments and samples being measured are generally solutions.

When using TGA to find the particle loading in the fiber, which was calculated to be 7% by volume, it was observed that the particles had an effect on the degradation profile compared to an alginate fiber without nanoparticles. The initial degradation temperature was delayed due to the high density of the particle loading, but sub sequential weight loss steps occurred at lower temperatures because of the decreased amount of alginate per filament of magnetic fiber than a pure alginate fiber.

For observation in the TEM, the particles were encapsulated within the fiber in linear aggregates of various sizes along the direction of the fiber formation. The loading, 7% by volume from TGA, of IONPs into alginate fibers had no significant effect on the extension, tenacity, and modulus of the fiber as compared to an alginate fiber spun in the same conditions without nanoparticles. This study is a proof of concept that magnetic fibers can be produced using existing technologies that are commonly used in the production of high performance fibers.

ACKNOWLEDGMENTS

Special thanks to Maeve Budi for synthesis of IONPs, Thomas Lawton for AC magnetic hyperthermia measurements, JoAn Hudson for sample preparation of fibers for TEM, Bin Qi for TEM images of particles and fibers, Longfei Ye and Thomas Crawford at the University of South Carolina Department of Physics and Astronomy for VSM data on fibers, James Lowe for assistance with tensile testing, and Kimberly Ivey for modulated DSC measurements. Funding for this project was provided by the National Textile Center (M10-Cl02).

REFERENCES

1. Terris, B. D.; Thomson, T. *J. Phys. D: Appl. Phys.* **2005**, *38*, R199.
2. Stone, R.; Willi, T.; Rosen, Y.; Mefford, O. T.; Alexis, F. *Ther. Deliv.* **2011**, *2*, 815.
3. Lu, A.; Salabas, E.; Schüth, F. *Angew. Chem. Int. Ed.* **2007**, *46*, 1222.
4. Tan, S.; Wendorff, J.; Pietzonka, C.; Jia, Z.; Wang, G. *ChemPhysChem* **2005**, *6*, 1461.
5. Andrew, J. S.; Clarke, D. R. *Langmuir* **2008**, *24*, 670.
6. Yang, D.; Lu, B.; Zhao, Y.; Jiang, X. *Adv. Mater.* **2007**, *19*, 3702.
7. Song, T.; Zhang, Y.; Zhou, T.; Lim, C.; Ramakrishna, S.; Liu, B. *Chem. Phys. Lett.* **2005**, *415*, 317.
8. Turek, K. *J. Magn. Magn. Mater.* **1990**, *83*, 279.
9. Mayes, E.; Vollrath, F.; Mann, S. *Adv. Mater.* **1998**, *10*, 801.
10. Behabtu, N.; Young, C. C.; Tsentalovich, D. E.; Kleinerman, O.; Wang, X.; Ma, A. W. K.; Bengio, E. A.; ter Waarbeek, R. F.; de Jong, J. J.; Hoogerwerf, R. E.; Fairchild, S. B.; Ferguson, J. B.; Maruyama, B.; Kono, J.; Talmon, Y.; Cohen, Y.; Otto, M. J.; Pasquali, M. *Science* **2013**, *339*, 182.
11. Qin, Y. *Polym. Int.* **2008**, *57*, 171.
12. Mikołajczyk, T.; Wołowska Czapnik, D.; Bogun, M. *J. Appl. Polym. Sci.* **2007**, *107*, 1670.
13. Sun, S.; Zeng, H.; Robinson, D.; Raoux, S.; Rice, P.; Wang, S.; Li, G. *J. Am. Chem. Soc.* **2004**, *126*, 273.
14. Khalafalla, S.; Reimers, G. *IEEE Trans. Magn.* **1980**, *16*, 178.
15. Mornet, S.; Vasseur, S.; Grasset, F.; Veverka, P.; Goglio, G.; Demourgues, A.; Portier, J.; Pollert, E.; Duguet, E. *Prog. Solid State Chem.* **2006**, *34*, 237.
16. Pankhurst, Q.; Connolly, J.; Jones, S.; Dobson, J. *J. Phys. D: Appl. Phys.* **2003**, *36*, R167.
17. Veverka, P.; Pollert, E.; Záveta, K.; Vasseur, S.; Duguet, E. *Nanotechnology* **2008**, *19*, 215705.